THE UNIVERSITY *of* EDINBURGH

Edinburgh Research Explorer

Weighted density functional theory for simple fluids: supercritical adsorption of a Lennard-Jones fluid in an ideal slit pore

OPEN ACCESS

Weighted density functional theory for simple fluids: Supercritical adsorption of a Lennard-Jones fluid in an ideal slit pore

M. B. Sweatman

Department of Chemistry, Imperial College of Science, Technology, and Medicine, London, SW7 2AZ, United Kingdom

The adsorption of a Lennard-Jones fluid in an ideal slit pore is studied using weighted density functional theory. The intrinsic Helmholtz free-energy functional is separated into repulsive and attractive contributions. Rosenfeld's accurate fundamental measure functional is employed for the repulsive functional while another weighted density functional method is employed for the attractive functional. This other method requires an accurate equation of state for the bulk fluid and an accurate pair-direct correlation function for a uniform fluid, determined analytically or numerically. The results for this theory are compared against mean-field density functional theory and grand canonical ensemble simulation results, modeling the adsorption of ethane in a graphite slit. The results indicate that the weighted density functional method applied to the attractive functional can offer a significant increase in accuracy over the mean-field theory.

I. INTRODUCTION

Considerable progress has been made in recent decades in the understanding of phenomena arising from the interaction of fluids with surfaces [1]. From a theoretical perspective, density functional theory (DFT) has played a significant part in this increasingly active field. In the past two decades, there have been rapid improvements in the accuracy of density functional methods that treat repulsive forces [2–8], but there has been little improvement in methods for treating attractive forces, e.g., the dispersion forces modelled by the Lennard-Jones (LJ) fluid. A popular method for constructing a density functional for such fluids is to separate the intrinsic excess Helmholtz free-energy functional, F_{ex}, into repulsive and attractive contributions,

$$F_{ex}[\rho(\vec{r})] = F_{rep}[\rho(\vec{r})] + F_{att}[\rho(\vec{r})] \qquad (1)$$

where $\rho(\vec{r})$ is the average one-body density and other notation is obvious. The pair potential, ϕ, is also separated into corresponding repulsive and attractive contributions,

$$\phi(r) = \phi_{rep}(r) + \phi_{att}(r). \qquad (2)$$

To achieve this separation, the prescriptions of Barker and Henderson (BH) [9] or Weeks, Chandler, and Anderson (WCA) [10] are often invoked. The repulsive functional is then usually approximated by a hard-sphere functional with an appropriate choice of hard-sphere diameter. The attractive functional is often treated in mean-field fashion. The result is that the approximation for the attractive functional is usually considerably less accurate than the approximation for the repulsive functional. At high temperatures, where the repulsive functional dominates fluid behavior, this is often not very important. But at lower temperatures it becomes more important that the attractive functional is accurate.

Several methods that attempt to improve upon the mean-field functional for attractive forces have been proposed. For the LJ fluid they include modification of the effective hard-sphere diameter [11,12] and modification of the form of the

"effective" attractive interaction [13]. For more general fluids they include truncated density expansions [14] and methods based on a perturbative scheme [15]. Another method due to van Swol and Henderson [16] is similar to the one presented in this work, the significant difference being the form of the weight function used to define a smoothed density. Whilst being effective for some applications, the accuracy of these approaches has rarely been compared or established for a wide range of temperatures, densities, and model pair potentials.

This work focuses on the construction of a weighted density functional method and application of this method to the attractive functional of the LJ fluid. The performance of this method is investigated by comparing results for a LJ fluid, modeling the supercritical adsorption of a model of ethane in a planar graphite slit, with mean-field theory and simulation.

II. THEORY

The WDA method is developed quite generally and could be used to describe both attractive and repulsive forces. However, it is recognized that the inherent approximations in this method will generally not be as accurate for repulsive forces as established repulsive functionals [e.g., the fundamental measure functional (FMF) for the hard-sphere fluid of Rosenfeld and other workers [4–8]] and so in this work the WDA method is applied to the attractive functional only.

The grand potential functional, $\Omega[\rho(\vec{r})]$, is defined such that [17]

$$\Omega[\rho(\vec{r})] = F_{id}[\rho(\vec{r})] + F_{ex}[\rho(\vec{r})]$$
$$- \int d\vec{r}\rho(\vec{r})[\mu(\rho_b) - V_{ext}(\vec{r})], \qquad (3)$$

where F_{id} is the exact ideal-gas Helmholtz free-energy functional, V_{ext} is the external potential and $\mu(\rho_b)$ is the reservoir fluid chemical potential which is determined by the reservoir (bulk) density, ρ_b. The ideal-gas functional is given by

$$F_{id}[\rho(\vec{r})] = \beta^{-1} \int d\vec{r} \rho(\vec{r}) (\ln[\Lambda^3 \rho(\vec{r})] - 1), \quad (4)$$

where Λ is the de Broglie thermal wavelength and $\beta^{-1} = k_B T$ is the inverse temperature. Minimization of Eq. (3) with respect to $\rho(\vec{r})$ for a given chemical potential

$$\left(\frac{\delta \Omega}{\delta \rho(\vec{r})} \right)_\mu = 0 \quad (5)$$

yields the Euler-Lagrange equation for the density profile

$$\rho(\vec{r}_1) = \rho_b \exp(-\beta[V_{ext}(\vec{r}_1) - \mu_{ex}(\rho_b)] + c^{(1)}(\vec{r}_1; \rho)), \quad (6)$$

where $c^{(1)}(\vec{r}; \rho)$ is the first functional derivative of $-\beta F_{ex}$ with respect to $\rho(\vec{r})$, and $\beta \mu_{ex}(\rho_b)$, the excess chemical potential of the bulk fluid, is equated with $-c^{(1)}(\rho_b)$. Given $\mu_{ex}(\rho_b)$ and V_{ext} as input, and an approximate excess free-energy functional, the approximate equilibrium density profile and adsorption can be determined [assuming $\delta^2 \Omega / \delta \rho(\vec{r}_1) \delta \rho(\vec{r}_2) > 0$ at equilibrium].

The adsorption is often of great importance, in both experimental and theoretical studies. For a planar geometry, the adsorption, Γ, is defined by the Gibbs adsorption equation on an isotherm

$$A\Gamma = -\left(\frac{\partial \Omega^{ex}}{\partial \mu} \right)$$

$$= \int d\vec{r} [\rho(\vec{r}) - \rho_b] - \left(\frac{\partial F^{ex}}{\partial \mu} \right)_{\rho(\vec{r})}$$

$$- \int d\vec{r} \left(\frac{\delta \Omega^{ex}}{\delta \rho(\vec{r})} \right)_\mu \left(\frac{\partial \rho(\vec{r})}{\partial \mu} \right), \quad (7)$$

where $\Omega^{ex} = \Omega + PV$ is the excess grand potential (note the superscript ex which denotes exess over bulk, rather than a subscript ex which denotes excess over ideal gas), P is the bulk pressure and V is the volume of the system. An approximate functional will properly satisfy the Gibbs adsorption equation if the last two terms on the right-hand side are zero, i.e., if F^{ex} is independent of the chemical potential (or density) of the bulk fluid and if Eq. (5) is satisfied. Then the observed adsorption, $\Gamma_0 = A^{-1} \int d\vec{r} (\rho(\vec{r}) - \rho_b)$, can be equated with Γ.

A. Density functional mean-field theory

The intrinsic excess Helmholtz free-energy can be expressed formally [2,17] by

$$\beta F_{ex}[\rho(\vec{r})] = \int_0^1 d\alpha(\alpha - 1) \int d\vec{r}_1 \int d\vec{r}_2 \rho(\vec{r}_1) \rho(\vec{r}_2) c^{(2)}$$

$$\times (\vec{r}_1, \vec{r}_2; \rho_\alpha)$$

$$= \beta F_{rep}[\rho(\vec{r})] + \int_0^1 d\alpha(\alpha - 1)$$

$$\times \int d\vec{r}_1 \int d\vec{r}_2 \rho(\vec{r}_1) \rho(\vec{r}_2) c_{att}^{(2)}(\vec{r}_1, \vec{r}_2; \rho_\alpha), \quad (8)$$

where α parametrizes a path between the zero-density fluid and $\rho(\vec{r})$ such that

$$\rho(\vec{r}; \alpha) = \alpha \rho(\vec{r}) \equiv \rho_\alpha \quad (9)$$

and the pair-direct correlation function, $c^{(2)}(\vec{r}_1, \vec{r}_2) = \delta c^{(1)}(\vec{r}_1) / \delta \rho(\vec{r}_2)$, is the second functional derivative of F_{ex} with respect to $\rho(\vec{r})$. Alternatively, for a fluid with two-body (pair-potential) forces only, it can also be shown that

$$F_{ex}[\rho(\vec{r})] = F_{rep}[\rho(\vec{r})]$$

$$+ \frac{1}{2} \int_0^1 d\alpha \int d\vec{r}_1 \int d\vec{r}_2 \rho(\vec{r}_1) \rho(\vec{r}_2) g^{(2)}$$

$$\times (\vec{r}_1, \vec{r}_2; \phi_\alpha) \phi_{att}(r_{12}), \quad (10)$$

where now α parametrizes a path between the repulsive contribution to the pair-potential and the full pair potential such that

$$\phi(r; \alpha) = \phi_{rep}(r) + \alpha \phi_{att}(r) \equiv \phi_\alpha \quad (11)$$

and $g^{(2)}(\vec{r}_1, \vec{r}_2; \phi_\alpha)$ is the pair-distribution function. DFMFT can be easily derived by setting $c_{att}^{(2)}(\vec{r}_1, \vec{r}_2; \rho_\alpha) = -\beta \phi_{att}(r_{12})$ in Eq. (8) or by setting $g^{(2)}(\vec{r}_1, \vec{r}_2; \phi_\alpha) = 1$ in Eq. (10). For simple fluids these approximations are exact in the asymptotic $r \to \infty$ limit; hence the terminology ''mean field.'' The excess Helmholtz free-energy functional becomes

$$F_{ex}[\rho(\vec{r})] = F_{rep}[\rho(\vec{r})]$$

$$+ \frac{1}{2} \int d\vec{r}_1 \int d\vec{r}_2 \rho(\vec{r}_1) \rho(\vec{r}_2) \phi_{att}(r_{12}). \quad (12)$$

DFMFT is simple to implement and gives reasonable results for a range of fluid phenomena. Consequently, it has found widespread application despite its crude assumption concerning the attractive part of the inhomogeneous fluid pair-direct correlation function, namely $c_{att}^{(2)}(\vec{r}_1, \vec{r}_2) = -\beta \phi_{att}(r_{12})$ for all fluid states. The bulk-fluid equation of state generated by this functional, with a suitable hard-sphere functional for F_{rep}, is not very accurate for the LJ fluid. For this reason, methods have been suggested that modify the effective hard-

sphere diameter entering F_{rep} [11,12], and sometimes ϕ_{att} [13], to improve the bulk equation of state (EOS). The prescription of Lu *et al.* [11] improves some aspects of the bulk thermodynamic properties of DFMFT for the LJ fluid at low temperatures, but it is not accurate in the region of the bulk critical temperature. The prescription of Walton and Quirke [12] fixes the hard-sphere diameter to guarantee that the chemical potential of the bulk fluid generated by the density functional theory agrees with an equation of state. While this prescription does not properly satisfy the Gibbs adsorption equation (7) because the repulsive functional is dependent on the bulk density through the hard-sphere diameter, the resulting inconsistency in Eq. (7) is presumably small in their application to supercritical adsorption. Velasco and Tarazona [13] have performed several studies of the adsorption of the LJ fluid with an *ad hoc* modification for the attractive interaction, ϕ_{att}. While this method has been shown to give reasonable results at subcritical temperatures for the adsorption of a Lennard-Jones fluid in planar geometries, it is not clear how this method can be applied more generally.

B. The WDA method

The WDA method is essentially a crude method for implementing a WDA functional for fluids for which an accurate equation of state is known but the pair-direct correlation function can be accurately determined by numerical methods only. The method presented in this work was first described in [21]. It is similar to the method of van Swol and Henderson [16] who constructed a WDA for the attractive functional of the square-well fluid. The work of Sokolowski and co-workers [22] also has some similarity in that a WDA is used to construct a functional for the associative contribution to the total Helmholtz free-energy of a model associating fluid.

The excess Helmholtz free-energy is approximated by a weighted density functional given by

$$F_{ex}[\rho(\vec{r})] = \int d\vec{r}\rho(\vec{r})\Psi_{ex}(\bar{\rho}(\vec{r})), \qquad (13)$$

where Ψ_{ex} is the excess Helmholtz free-energy per particle of a bulk fluid with density $\bar{\rho}$. The weighted density, $\bar{\rho}(r)$, is defined by

$$\bar{\rho}(\vec{r}_1) = \int d\vec{r}_2\rho(\vec{r}_2)w(r_{12};\bar{\rho}(\vec{r}_1)), \qquad (14)$$

where $w(r_{12};\rho(\vec{r}_1))$ is a normalized, density-dependent weight function. The weight function is itself determined by requiring the functional to generate accurate pair-direct correlation functions for all uniform densities, i.e.,

$$-\beta^{-1}c^{(2)}(r_{12};\rho) = \Psi'_{ex}\left(\frac{\delta\bar{\rho}(\vec{r}_1)}{\delta\rho(\vec{r}_2)} + \frac{\delta\bar{\rho}(\vec{r}_2)}{\delta\rho(\vec{r}_1)}\right)$$
$$+ \rho\Psi''_{ex}\int d\vec{r}_3 \frac{\delta\bar{\rho}(\vec{r}_3)}{\delta\rho(\vec{r}_1)}\frac{\delta\bar{\rho}(\vec{r}_3)}{\delta\rho(\vec{r}_2)}$$
$$+ \rho\Psi'_{ex}\int d\vec{r}_3 \frac{\delta^2\bar{\rho}(\vec{r}_3)}{\delta\rho(\vec{r}_1)\delta\rho(\vec{r}_2)}, \quad (15)$$

where $'$ and $''$ indicate the first and second derivatives with respect to density and all quantities are evaluated for a uniform density. Thus, in Eq. (15)

$$\frac{\delta\bar{\rho}(\vec{r}_1)}{\delta\rho(\vec{r}_2)} = \frac{\delta\bar{\rho}(\vec{r}_2)}{\delta\rho(\vec{r}_1)} = w(r_{12};\rho),$$

$$\frac{\delta^2\bar{\rho}(\vec{r}_3)}{\delta\rho(\vec{r}_1)\delta\rho(\vec{r}_2)} = w'(r_{13};\rho)w(r_{23};\rho) + w'(r_{23};\rho)w(r_{13};\rho).$$
$$(16)$$

When Ψ_{ex} and $c^{(2)}(r)$ can be approximated analytically, then with a suitable approximation for the density dependence of $w(r;\rho)$, Eqs. (15) and (16) can be solved to find $w(r;\rho)$. This is essentially the approach used by Tarazona in [4]. When the bulk-fluid pair direct correlation function can be determined approximately only at n nonzero density points the weight function can be expanded to nth order in density

$$w(r;\rho) = \sum_{i=0}^{n} \rho^n w_i(r). \qquad (17)$$

Because it becomes increasingly difficult to find the solution set of weight functions, w_i, as n increases, this work employs a linear approximation for w, i.e.,

$$w(r;\rho) = w_0(r) + \rho w_1(r). \qquad (18)$$

With an analytic approximation for Ψ_{ex} and with $c^{(2)}(r)$ determined approximately at one nonzero bulk density, ρ_1, the system of equations (15), (16), and (18) can be solved at ρ_1. The weight functions are given by

$$w_0(r) = -\beta c^{(2)}(r;\rho=0)/2\Psi'_{ex}(\rho=0),$$

$$w_1(k) = [-b + (b^2 - 4ac)^{1/2}]/2a,$$

$$a = \rho_1^3\Psi''_{ex}(\rho_1) + 2\rho_1^2\Psi'_{ex}(\rho_1),$$

$$b = 2\rho_1^2\Psi''_{ex}(\rho_1)w_0(k) + 2\rho_1\Psi'_{ex}(\rho_1)[1 + w_0(k)],$$

$$c = \rho_1\Psi''_{ex}(\rho_1)w_0(k)^2 + 2\Psi'_{ex}(\rho_1)w_0(k) + \beta c^{(2)}(k;\rho_1),$$
$$(19)$$

where k indicates the Fourier transformed quantity. It is assumed that the linear approximation (18) is sufficiently accurate for densities other than ρ_1, i.e., that with Eq. (18) $c^{(2)}(\vec{r}_1,\vec{r}_2)$ is sufficiently accurate for all densities $\rho(\vec{r})$. These equations require that Ψ_{ex} is consistent with $c^{(2)}(r;\rho_1)$. For example, for hard-spheres the PY solution [23] for these quantities can be used. The presence of the square-root term indicates that Eq. (19) might not have real solutions for some fluid systems. In this work no such difficulties are encountered for the LJ fluid.

Finally, the remaining parameter ρ_1 must be determined. In this work, an *ad hoc* relation is suggested

$$\rho_1 = \frac{\int d\vec{r} |\nabla \rho(\vec{r})| \bar{\rho}(\vec{r})}{\int d\vec{r} |\nabla \rho(\vec{r})|}. \qquad (20)$$

This forces the functional to generate accurate $c^{(2)}(r)$ for uniform densities close to $\bar{\rho}(\vec{r}\,')$ where $\vec{r}\,'$ is the position in the fluid where the structure is most inhomogeneous. With this choice for ρ_1 the complete functional avoids reference to the bulk fluid, which could lead to thermodynamic inconsistencies [24].

In this work the functional described above is employed for the attractive functional of the LJ fluid only, with the hard-sphere FMF employed for the repulsive functional. Thus, all occurences F_{ex}, Ψ_{ex} and $c^{(2)}$ in Eqs. (13) to (19) should be exchanged for F_{att}, Ψ_{att} and $c_{att}^{(2)}$ respectively. Since the repulsive functional is approximated by Rosenfeld's hard-sphere FMF [6], $\Psi_{att} = \Psi - \Psi_{PYHS}$ and $c_{att}^{(2)} = c^{(2)} - c_{PYHS}^{(2)}$, where the hard-sphere (PYHS) functions are calculated using the same hard-sphere diameter as used in the repulsive functional.

However, the Lennard-Jones fluid has more complex behavior than the hard-sphere fluid and there does not yet exist an accurate analytic EOS for this system that is also consistent with accurate pair-direct correlation functions. To force a solution to Eq. (19) the input $c_{att}^{(2)}(\rho_1)$ is manipulated by simply scaling it by an appropriate factor so that it does agree with Ψ_{att}. It will be seen that this crude manipulation is sufficient to produce accurate results for supercritical adsorption.

Thus the complete description for this WDA method is given by Eqs. (13), (14), (18)–(20). As with Tarazona's hard-sphere functional [4] (as opposed to Rosenfeld's FMF for hard-spheres [6]), the above method uses three-dimensional bulk fluid data as input in its construction. Thus, this functional cannot be expected to be very accurate as the effective dimensionality of the nonuniform fluid is significantly reduced.

As with many other WDA functionals, this WDA method generates direct correlation functions to all orders, i.e., for a general fluid

$$\frac{-\beta \delta^n F_{ex}}{\delta \rho(\vec{r}_1) \delta \rho(\vec{r}_2), \ldots, \delta \rho(\vec{r}_n)} = c^{(n)}(\vec{r}_1, \vec{r}_2, \ldots, \vec{r}_n) \neq 0 \qquad (21)$$

for $n \geq 0$. This is not achieved by second-order approaches such as DFMFT and the method of Velasco and Tarazona [13] or by truncated density expansion approaches [14] (by definition, truncated density expansion theories generate direct correlation functions up to the order of truncation only).

The accuracy of a DFT method can be estimated by examining $c^{(n)}$ generated for uniform fluids. For this WDA method, the accuracy of $c^{(0)}$ and $c^{(1)}$ for a uniform fluid are determined by the accuracy of the equation-of-state, Ψ. The method generates accurate pair-direct correlation functions for uniform fluid states close to $\rho = 0$ and $\rho = \rho_1$ (assuming that the input $c^{(2)}(\rho_1)$ is accurate) and so is likely to produce

reasonably accurate fluid structure for an inhomogeneous fluid. Thus this WDA approach is likely to be more accurate than the perturbation approaches [15] based on the expression (10). These approaches are not accurate for dense fluids [16,25] because they overemphasize structure in pair-direct correlaion functions for dense fluids. A similar criticism can also be leveled at the method of Velasco and Tarazona [13]. These authors modify the prescription for the effective hard-sphere diameter, d, and the form of the attractive pair-potential, $\phi_{att}(r)$, entering Eq. (12) so that accurate densities for coexisting bulk liquid and gas phases are generated by the resulting DFT. They choose an *ad hoc* modification for $\phi_{att}(r)$ by considering the perturbation expression (10). As with the perturbation approaches [15], their approach tends to overemphasize attractive pair correlations in dense fluids [21]. Returning to the WDA method, the form of uniform-fluid direct correlation functions, $c^{(n)}$, for $n > 2$ is not controlled, although their magnitude (given by integration over $n-1$ spatial dimensions) is determined by Ψ.

If all terms in Eq. (23) are evaluated explicitly, then this WDA method will satisfy the Gibbs adsorption equation and yield consistent and reasonably accurate values for thermodynamic quantities. This is generally not achieved by the truncated density expansion approaches [14] as explained in [24].

This WDA method is qualitatively similar to the approach of van-Swol and Henderson [16]. Their theory is also expressed by Eqs. (13) and (14), but they choose a less accurate expression for $w(r; \rho)$ than employed in this work. In particular, they do not enforce the requirements (18)–(20). It is emphasized that these requirements are important for generating accurate structure in the inhomogeneous fluid. Rather, they interpolate $w(r; \rho)$ between the exact low density limit [$w_0(r)$ in the method of this work] and a mean-field weight-function equal to the normalized attractive potential, i.e.,

$$w(r; \rho) = a(\rho) w_0(r) + [1 - a(\rho)] \frac{\phi_{att}(r)}{\int d\vec{r} \phi_{att}(r)}, \qquad (22)$$

where a is an *ad hoc* density-dependent switching function.

Given the above features and the good performance of Tarazona's hard-sphere functional [4] and the functional for the square-well fluid of van Swol and Henderson [16], it is likely that the method in this work will be reasonably accurate for a wide range of fluids and fluid states whenever the required input data [Ψ_{ex} and $c^{(2)}(\rho_1)$] is accurate.

Since ρ_1 is dependent on $\rho(\vec{r})$, the first derivative of F_{ex} with respect to $\rho(\vec{r})$ becomes

$$\left(\frac{\delta F_{ex}}{\delta \rho(\vec{r})} \right)_\mu = \left(\frac{\delta F_{ex}}{\delta \rho(\vec{r})} \right)_{\mu, \rho_1} + \left(\frac{\partial F_{ex}}{\partial \rho_1} \right)_{\mu, \rho(\vec{r})} \left(\frac{\delta \rho_1}{\delta \rho(\vec{r})} \right)_\mu. \qquad (23)$$

Because $\partial^n F_{ex} / \partial \rho_1^n$ evaluated for a uniform density is zero for all n, the last term on the right of Eq. (23) is zero for a uniform fluid. Also, no additional terms appear in Eq. (15) which gives the pair-direct correlation function for a uniform

fluid. For a nonuniform fluid, the last term on the right of Eq. (23) will generally be nonzero. But in this work it is assumed that this term is almost zero. Thus the condition for equilibrium becomes

$$\left(\frac{\delta\Omega}{\delta\rho(\vec{r})}\right)_{\mu,\rho_1} = 0, \tag{24}$$

i.e., it is assumed that

$$\left(\frac{\delta\Omega}{\delta\rho(\vec{r})}\right)_{\mu} = \left(\frac{\partial F_{ex}}{\partial\rho_1}\right)_{\mu,\rho(\vec{r})}\left(\frac{\delta\rho_1}{\delta\rho(\vec{r})}\right)_{\mu} \approx 0. \tag{25}$$

It will be demonstrated that the above assumption is reasonable for the application to supercritical adsorption in this work. It is emphasized that in principle all terms in Eq. (23) could be evaluated explicitly.

By rewriting Eq. (13) as

$$F_{ex}[\rho(\vec{r})] = \int d\vec{r}_1 \int d\vec{r}_2 \rho(\vec{r}_1)\rho(\vec{r}_2)\Xi_{ex}(r_{12};\bar{\rho}(\vec{r}_1)), \tag{26}$$

where

$$\bar{\rho}(\vec{r}_1)\Xi_{ex}(r_{12};\bar{\rho}(\vec{r}_1)) = \Psi_{ex}(\bar{\rho}(\vec{r}_1))w(r_{12};\bar{\rho}(\vec{r}_1)) \tag{27}$$

it can be seen that Eq. (13) can be obtained by setting

$$\int_0^1 d\alpha(\alpha-1)c^{(2)}(\vec{r}_1,\vec{r}_2;\rho_\alpha) = \frac{\beta\Psi_{ex}(\bar{\rho}(\vec{r}_1))}{\bar{\rho}(\vec{r}_1)}w(r_{12};\bar{\rho}(\vec{r}_1)) \tag{28}$$

in Eq. (8). This shows that the approximation (13) has broken the symmetry of $c^{(2)}(\vec{r}_1,\vec{r}_2)$ with respect to interchange of $\vec{r}_1$ and $\vec{r}_2$, and it immiediately suggests that a possible improvement to Eq. (13) can be written as

$$F_{ex}[\rho(\vec{r})] = \int d\vec{r}_1 \int d\vec{r}_2 \rho(\vec{r}_1)\rho(\vec{r}_2)\Xi_{ex}(r_{12};\hat{\rho}(\vec{r}_1,\vec{r}_2)), \tag{29}$$

where $\hat{\rho}(\vec{r}_1,\vec{r}_2) = (\bar{\rho}(\vec{r}_1)+\bar{\rho}(\vec{r}_2))/2$. Nevertheless, in this work the WDA (13) rather than Eq. (29) is employed.

III. SUPERCRITICAL ADSORPTION IN A PLANAR SLIT

The supercritical adsorption of a Lennard-Jones fluid in an ideal slit is investigated using the two theories described in the previous section. The fluid-fluid and surface-fluid interaction parameters are chosen to model the interaction of ethane with graphite. This system has been studied previously by Walton and Quirke [12], van Megan and Snook [18] and Tan and Gubbins [19] using both simulation and DFT methods. Such systems are commonly studied, for example, in application to gas adsorption in, and characterization of, porous materials [26].

For each application in this work the intrinsic excess Helmholtz free-energy functional for the LJ fluid is separated

into repulsive and attractive contibutions (1). The LJ pair potential,

$$\phi_{LJ}(r) = 4\epsilon((r^*)^{-12}-(r^*)^{-6}); \quad r^*=r/\sigma, \tag{30}$$

where σ and ϵ establish the length and energy scales of the potential, is then separated according to the WCA prescription [10], i.e., the LJ pair potential is split at its minimum, $\phi(r_{min})=-\epsilon$, with $r_{min}=2^{1/6}\sigma$

$$\phi_{rep}^{LJ}(r) = \phi_{LJ}(r)+\epsilon; \quad r\leqslant r_{min}=0; \quad r>r_{min},$$

$$\phi_{att}^{LJ}(r) = -\epsilon; \quad r\leqslant r_{min} = \phi_{LJ}(r); \quad r>r_{min}. \tag{31}$$

The repulsive functional is approximated by the FMF for hard spheres of Rosenfeld and of Kierlik and Rosinberg [6]. This functional is not described in this work since it has been well documeted elsewhere. The effective hard-sphere diameter, d, entering the hard-sphere functional is calculated according to the Barker-Henderson (BH) prescription [9],

$$d = \int dr(1-\exp[-\beta\phi_{rep}(r)]), \tag{32}$$

which is the low-density limit of the WCA prescription [20]. Since Eq. (32) is independent of ρ_b, the repulsive functional properly satisfies the Gibbs adsorption equation (7).

Ethane is modeled by a Lennard-Jones potential (30), truncated and shifted at $r_c^*=2.5$

$$\phi_{att}(r) = \phi_{att}^{LJ}(r)-\phi_{LJ}(r_c); \quad r\leqslant r_c=0; \quad r>r_c. \tag{33}$$

The graphite surface is modeled by a Steele 10-4-3 potential [27], devoid of structure in directions parallel to the surface,

$$V_s(z) = \epsilon_w\left[\frac{4}{10}\left(\frac{\sigma_w}{z}\right)^{10}-\left(\frac{\sigma_w}{z}\right)^4-\frac{\sigma_w^4}{3\Delta(z+0.61\Delta)^3}\right]; \quad z>0, \tag{34}$$

with values for the parameters $\sigma_w=0.903\sigma$, $\epsilon_w=12.96\epsilon$, and $\Delta=0.8044\sigma$. For a planar slit of width H, $V_{ext}(z)=V_s(z)+V_s(H-z)$.

Tan and Gubbins and van Megan and Snook modeled this system at the supercritical reduced temperature $T^*=k_bT/\epsilon=1.35$ using computer simulation, but they obtained slightly different results. Consequently, for this work Grand canonical ensemble simulation has been used to obtain a new set of computer simulation results for this system.

Application of the WDA method to the attractive functional requires the definition of Ψ_{att} and $c_{att}^{(2)}(\rho_1)$ for the bulk fluid under consideration. There are several equations that describe the bulk thermodynamic properties of the LJ fluid. In this work the equation-of-state of Kolafa and Nezbeda [28] is used since it has the advantage that it is exact in the low density limit. A mean-field correction is applied to this equation-of-state to account for truncation and shifting of the LJ pair potential
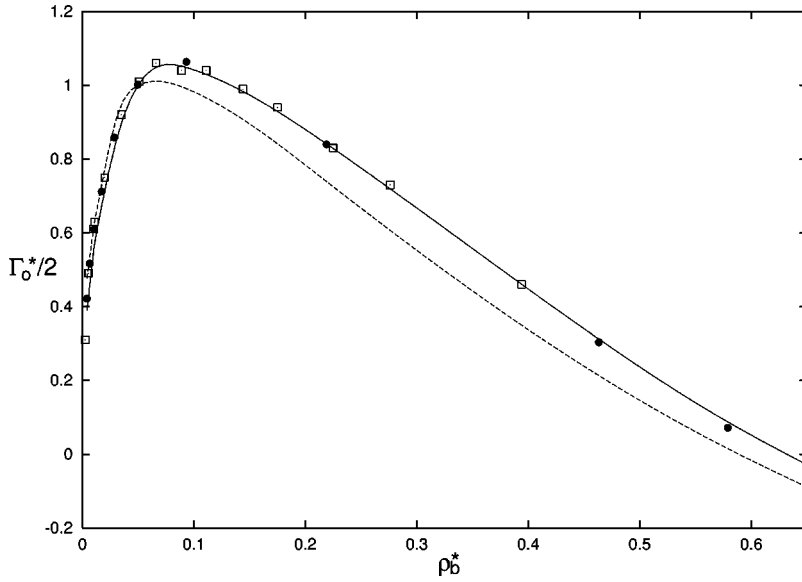
FIG. 1. Observed adsorption isotherms for a model of ethane in a graphite slit at $T^* = 1.35$ and $H^* = 5$. The solid line, dashed line, solid symbols and open symbols are the results of the WDA method of this work, DFMFT, the GCEMC simulations of this work and the GCEMC simulations of van Megan and Snook, respectively.

$$\Psi_{att}(\rho) = \Psi_{LJ}(\rho) - \Psi_{PY}(\rho;d) - \frac{\rho}{2} \int_0^{r_c} d\vec{r}\, \phi_{LJ}(r_c)$$
$$- \frac{\rho}{2} \int_{r_c}^{\infty} d\vec{r}\, \phi_{LJ}(r), \quad (35)$$

$$c_{att}^{(2)}(r;\rho_1) = [c_{HNC}^{(2)}(r;\rho_1) - c_{PY}^{(2)}(r;\rho_1;d)]$$
$$\times \left(\frac{-2\beta\Psi'_{att}(\rho_1) - \beta\rho_1\Psi''_{att}(\rho_1)}{c_{HNC}^{(2)}(k=0;\rho_1) - c_{PY}^{(2)}(k=0;\rho_1;d)} \right), \quad (36)$$

where Ψ_{LJ} and Ψ_{PY} denote the equation-of-state of Kolafa and Nezbeda and the Percus-Yevick compressibility equation of state for hard spheres [23], respectively.

Similarly, there are many methods for generating $c_{att}^{(2)}(\rho_1)$, but none are exactly consistent with the equation of state of Kolafa and Nezbeda. In this work the Hyper-netted-chain (HNC) integral equation closure [20] is employed to generate $c_{att}^{(2)}(\rho_1)$, and a scaling method [using Eq. (15)] is used to enforce consistency, i.e.,

where $c_{HNC}^{(2)}$ and $c_{PY}^{(2)}$ denote the pair-direct correlation functions resulting from solution of the HNC equation [for the truncated potential (33)] and the PY equation for hard spheres [23], respectively, and k denotes the fourier transformed quantity. The weight functions resulting from Eq. (19) are truncated at r_c and manipulated to ensure $w_0(k=0) = 1$ and $w_1(k=0) = 0$ (w_0 is rescaled and w_1 is shifted). Finally, in all cases, a grid of 50 points per σ and simple Picard iteration is used to solve the respective Euler-Lagrange equations.
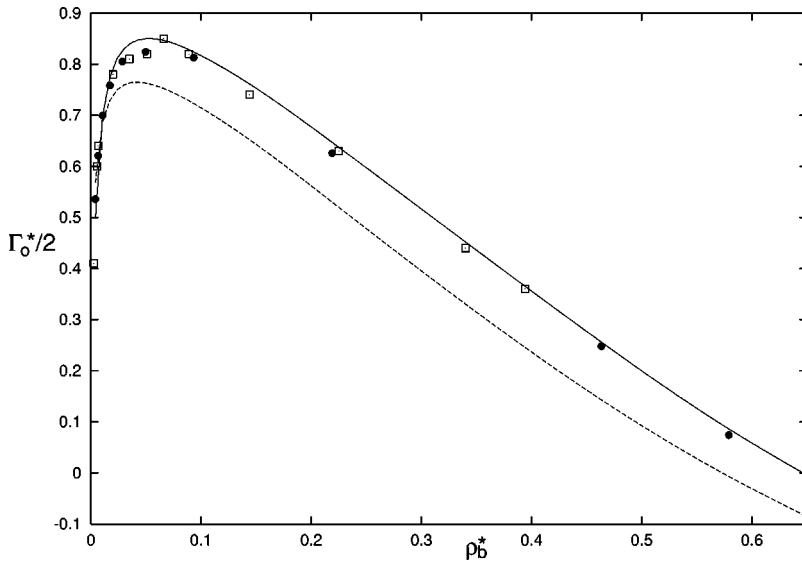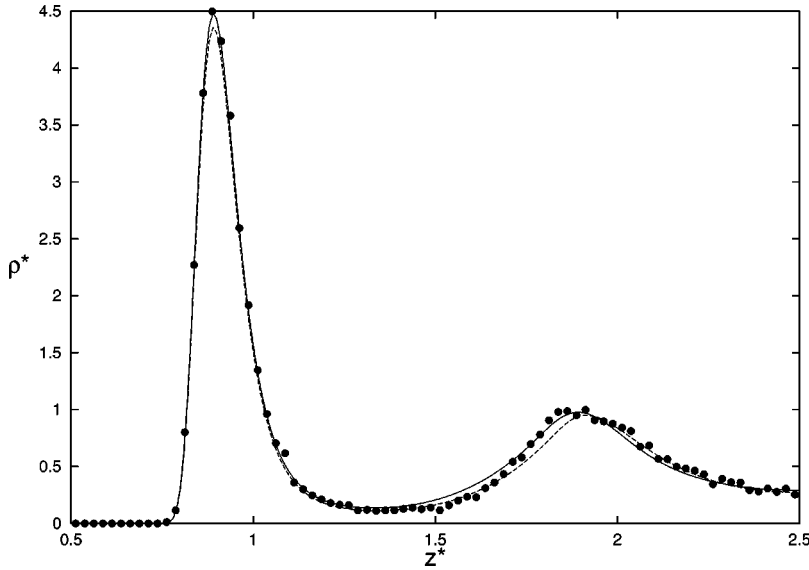

FIG. 2. As for Fig. 1 except that $H^* = 3.5$.

FIG. 3. Half-slit density profiles corresponding to the same system as in Fig. 1. The bulk density $\rho_b^*=0.09334$ corresponds closely to that at which the adsorption is a maximum. The key is the same as in Fig. 1.

Figure 1 shows the variation of the reduced observed adsorption, $\Gamma_0^*=\Gamma_0\sigma^2$, with reduced bulk density, $\rho_b^*=\rho_b\sigma^3$, at $T^*=1.35$ and with $H^*=H/\sigma=5$ using simulation and DFT methods. Figure 2 shows the same system but with $H^*=3.5$. The new simulation results agree with those of van Megan and Snook, but not with those of Tan and Gubbins for $H^*=5$ (incidentally, the simulation results of Tan and Gubbins for $H^*=5$ can be closely reproduced with the simulation code employed in this work if the fluid-fluid potential is cut but *not* shifted). These figures show that the WDA method applied to the attractive functional of the LJ fluid is more accurate than the mean-field method for generation of supercritical adsorption isotherms. With the WDA method, the adsorption isotherms show a maximum characteristic of supercritical adsorption and are in good agreement with the simulation results of this work. The mean-field theory is less accurate, consistently overpredicting adsorption at low bulk densities and under-predicting adsorption at high bulk densities. It should also be noted that in the work of Tan and Gubbins good agreement was found between their simulation results and DFMFT using the effective hard-sphere diameter of Lu *et al.* The accuracy of DFMFT with the prescription of Lu *et al.* [11] should be reappraised for the supercritical LJ fluid in the light of these new simulation results, and the simulation results of van Megan and Snook.

Figures 3 and 4 show the density profiles resulting from simulation and theory corresponding to bulk densities of $\rho_b^*=0.0933$ and $\rho_b^*=0.0497$ with $H^*=5$ and $H^*=3.5$, respectively (note that $z^*=z/\sigma$). It can be seen that the WDA method is more accurate than DFMFT, although DFMFT is almost as accurate as the WDA method in Fig. 3.

Since in this work it has been assumed that Eq. (25) holds, then the WDA method does not properly satisfy the Gibbs adsorption equation. This can be seen by writing a
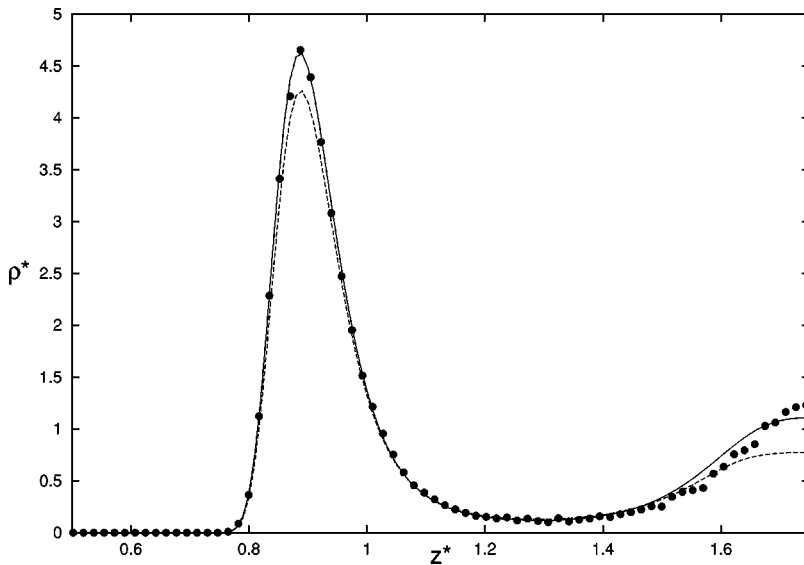

FIG. 4. Half-slit density profiles corresponding to the same system as in Fig. 2. The bulk density $\rho_b^*=0.0497$ corresponds closely to that at which the adsorption is a maximum. The key is the same as in Fig. 2.
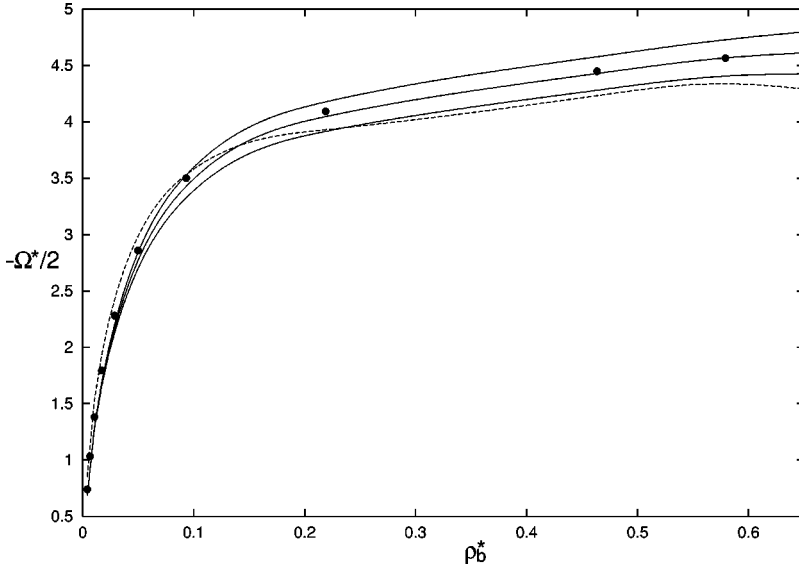
FIG. 5. Excess grand potential isotherms corresponding to the same system as in Fig. 1. The upper and lower solid lines correspond to the excess grand potential calculated from the grand potential functional of the WDA method and by integrating the observed adsorption isotherm of the WDA method, respectively. The middle solid line is the average of these results. The dashed line and symbols correspond to the results of DFMFT and the simulations of this work, respectively.

change in the grand potential as

$$-\Delta\Omega^{ex} = -\int \left(\frac{\partial\Omega^{ex}}{\partial\mu}\right)_{\rho(\vec{r})} d\mu - \int \left(\frac{\delta\Omega^{ex}}{\delta\rho(\vec{r})}\right)_{\mu} d\rho(\vec{r})$$

$$= \int\int [\rho(\vec{r})-\rho_b]d\vec{r}d\mu - \int \left(\frac{\delta\Omega^{ex}}{\delta\rho(\vec{r})}\right)_{\mu,\rho_1} d\rho(\vec{r})$$

$$- \int \left(\frac{\partial\Omega^{ex}}{\partial\rho_1}\right)_{\mu,\rho(\vec{r})} d\rho_1. \qquad (37)$$

Since the condition for equilibrium is given by Eq. (25), for the WDA method applied to the attractive functional of the LJ fluid this becomes

$$-\Delta\Omega^{ex} = A\int \Gamma_0 d\mu - \int \left(\frac{\partial F_{att}}{\partial\rho_1}\right)_{\mu,\rho(\vec{r})} d\rho_1. \qquad (38)$$

The magnitude of the right-most term in Eq. (38) can be determined by comparing the excess grand potential isotherms determined from the grand potential functional with those generated by simply integrating the observed adsorption, Γ_0, with respect to the chemical potential. The resulting difference is equal to the right-most term in Eq. (38). Figures 5 and 6 show the results of such calculations for $H^*=5$ and $H^*=3.5$, respectively. In these figures the reduced excess grand potential $\Omega^* = \Omega^{ex}\sigma^2/A\epsilon$, the upper solid line is the result obtained from the grand potential functional of the WDA method, the lower solid line is the result obtained by integrating the observed adsorption, Γ_0, of the WDA method and the middle solid line corresponds to the average of these two routes. The symbols indicate the excess grand potential obtained by integrating the simulation adsorption isotherm [the integration constant, $\Omega^{ex}(\rho_b^*=0.00407)$, is interpolated from the values given by the two DFT methods]. Each of the solid lines is generally closer to the simulation results than the mean-field result, indicated by the dashed line. Also, in Figs. 5 and 6 the upper and lower solid lines bracket the
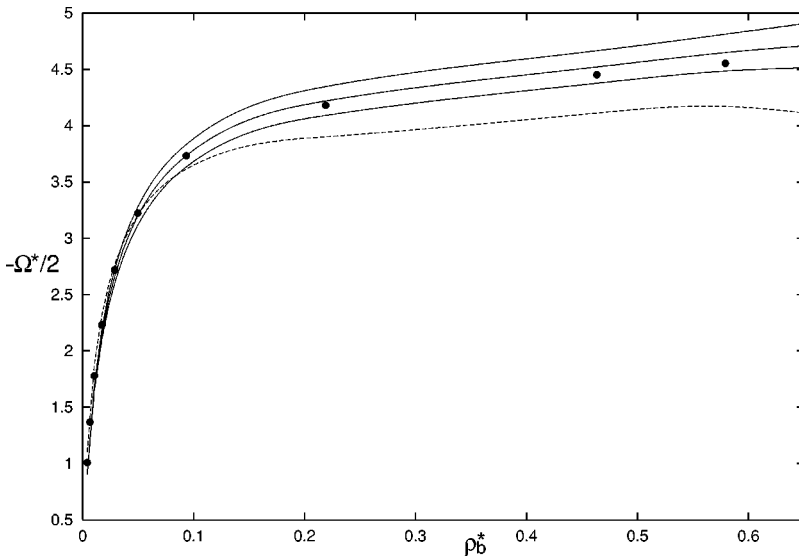

FIG. 6. As for Fig. 5 except that $H^*=3.5$.

simulation results. This provides some justification for neglecting terms of order $\partial F_{att}/\partial \rho_1$ in Eq. (23). At lower temperatures, where the attractive functional becomes more significant, neglect of such terms is less likely to be justified.

IV. CONCLUSION

It has been demonstrated that the WDA method applied to the attractive functional is more accurate than DFMFT for supercritical adsorption of a Lennard-Jones fluid in a model slit pore. It is expected that this accuracy extends to a wide range of regimes, and to other fluids where both an equation of state and accurate pair-direct correlation functions are available (analytically or numerically) for the bulk fluid. It is also possible to apply this method to the test-particle limit, with the modification $\rho_1 = \rho_b$, to generate pair correlation functions. Neglect of terms of order $\partial F_{att}/\partial \rho_1$ has been justified for the supercritical adsorption of the LJ fluid, although this neglect is unlikely to be justified at subcritical temperatures. The increase in accuracy of the WDA method over DFMFT has been gained at the expense of considerable additional complexity.

A problem with the new WDA method can occur if ρ_1 is inside the unstable spinodal region of the bulk phase diagram corresponding to the method used to obtain $c^{(2)}(\rho_1)$ used as input. When ρ_1 is within this region it will not be possible to obtain accurate values for $c^{(2)}(\rho_1)$, rendering the WDA method inaccurate. This is a consequence of using bulk-fluid information to construct a theory for the inhomogeneous fluid. This problem is under investigation.

[1] See, for example, *Fluid Interfacial Phenomena*, edited by C.A. Croxton (Wiley, New York, 1986); J.S. Rowlinson and B. Widom, *Molecular Theory of Capillarity* (Oxford University Press, New York, 1982); *Fundamentals of Inhomogeneous Fluids*, edited by D. Henderson (Wiley, New York, 1992).

[2] For a review, see R. Evans, in *Fundamentals of Inhomogeneous Fluids*, edited by D. Henderson (Wiley, New York, 1992).

[3] S. Nordholm, M. Johnson, and B.C. Freasier, Aust. J. Chem. **33**, 2139 (1980); M. Johnson and S. Nordholm, J. Chem. Phys. **75**, 1953 (1981).

[4] P. Tarazona and R. Evans, Mol. Phys. **52**, 847 (1984); P. Tarazona, Phys. Rev. A **31**, 2672 (1985); Z. Tan, G.S. Gubbins, U. Marini Bettolo Marconi, and F. van Swol, J. Chem. Phys. **90**, 3704 (1989).

[5] W.A. Curtin and N.W. Ashcroft, Phys. Rev. A **32**, 2909 (1985); A.R. Denton and N.W. Ashcroft, *ibid.* **42**, 7312 (1990).

[6] Y. Rosenfeld, Phys. Rev. Lett. **63**, 980 (1989); E. Kierlik and M.L. Rosinberg, Phys. Rev. A **42**, 3382 (1990); S. Phan, E. Kierlik, M.L. Rosinberg, B. Bildstein, and G. Kahl, Phys. Rev. E **48**, 618 (1993).

[7] Y. Rosenfeld, M. Schmidt, H. Lowen, and P. Tarazona, J. Phys.: Condens. Matter **8**, L577 (1996); Phys. Rev. E **55**, 4245 (1997).

[8] P. Tarazona, Phys. Rev. Lett. **84**, 694 (2000).

[9] J.A. Barker and D. Henderson, J. Chem. Phys. **47**, 4714 (1967).

[10] J.D. Weeks, D. Chandler, and H.C. Andersen, J. Chem. Phys. **54**, 5237 (1971); **54**, 5422 (1971).

[11] B.Q. Lu, R. Evans, and M.M. Telo da Gama, Mol. Phys. **55**, 1319 (1985).

[12] J.P.R.B. Walton and N. Quirke, Chem. Phys. Lett. **129**, 382 (1986).

[13] E. Velasco and P. Tarazona, J. Chem. Phys. **91**, 7916 (1989); Phys. Rev. A **42**, 2454 (1990).

[14] For example, see J.G. Powles, G. Rickayzen, and M.L. Williams, Mol. Phys. **64**, 33 (1988); Y. Rosenfeld, J. Chem. Phys. **98**, 8126 (1993); S.C. Kim and S.H. Suh, Phys. Rev. E **56**, 2889 (1997); N. Choudhury and S.K. Ghosh, J. Chem. Phys. **110**, 8628 (1999); C.N. Patra and A. Yethiraj, J. Phys. Chem. B **103**, 6080 (1999).

[15] For example, see L. Mederos, E. Chacon, G. Navascues, and M. Lombardero, Mol. Phys. **54**, 211 (1985); Z. Tang, L.E. Scriven, and H.T. Davis, J. Chem. Phys. **95**, 2659 (1991); S. Sokolowski and J. Fischer, *ibid.* **96**, 5441 (1992); S.C. Kim, J. Phys.: Condens. Matter **8**, 959 (1996).

[16] F. van Swol and J.R. Henderson, Phys. Rev. A **43**, 2932 (1991).

[17] R. Evans, Adv. Phys. **28**, 143 (1979).

[18] W. van Megan and I.K. Snook, Mol. Phys. **54**, 741 (1985).

[19] Z. Tan and K.E. Gubbins, J. Phys. Chem. **94**, 6061 (1990).

[20] J.P. Hansen and I.R. McDonald, *Theory of Simple Liquids* (Academic, London, 1986).

[21] M.B. Sweatman, Ph.D. thesis, University of Bristol, 1995.

[22] M. Borowko, K. Stepniak, S. Sokolowski, and R. Zagorski, Czech. J. Phys. **49**, 1067 (1999); K. Stepniak, A. Patrykiwjew, Z. Sokolowska, and S. Sokolowski, J. Colloid Interface Sci. **214**, 91 (1999); A. Patrykiwjew and S. Sokolowski, J. Phys. Chem. B **103**, 4466 (1999).

[23] J.L. Lebowitz, Phys. Rev. **133**, A895 (1964).

[24] M.B. Sweatman, Mol. Phys. **98**, 573 (2000).

[25] S. Varga, D. Boda, D. Henderson, and S. Sokolowski, J. Colloid Interface Sci. **227**, 223 (2000).

[26] For example, see S. Scaife, P. Kluson, and N. Quirke, J. Phys. Chem. B **104**, 313 (1999), and references therein.

[27] W.A. Steele, Surf. Sci. **36**, 317 (1973); *The Interaction of Gases with Solid Surfaces* (Pergamon, Oxford, 1974).

[28] J. Kolafa and I. Nezbeda, Fluid Phase Equilibria **100**, 1 (1994).